DOI: https://doi.org/10.4038/sljp.v24i1.8107

INSTITUTE OF PHYSICS – SRI LANKA

Research Article

Theoretic impetuses and lengths of Feinberg-Horodecki equation

C.A. Onate[1,*], D.T. Bankole[1], A.S. Olayinka[2] and O.E. Odeyemi[3].
[1]Department of Physical Sciences, Landmark University, Omu-Aran, Nigeria.
[2]Physics Department, Edo University, Iyamoh, Edo state, Nigeria.
[3]Department of Science Laboratory Technology, Federal College of Animal Health and Production Technology Apata, Ibadan, Nigeria.
Department of Physics, Faculty of Science, University of Colombo, Colombo 03, Sri Lanka

Abstract

The exact solution of the Feinberg-Horodecki equation for time-dependent harmonic vector potential has been investigated under a one-dimensional system. The quantized momentum and its corresponding un-normalized wave functions were explicitly obtained. The Fisher information (for time and momentum) and variance (for time and momentum) were calculated using expectation values of time and momentum via Hellman-Feynman Theory (HFT). The time and momentum Shannon entropy were obtained using an existing formula. Numerical results were for time and momentum Fisher information to confirm the Cramer-Rao inequality. Another numerical results were obtained for time and momentum Shannon entropy to confirm Bialynick-Birula, Mycielski (BBM) inequality. The effects of the potential parameters such as mass of the spring and the frequency on the theoretic quantities were fully examined. The new variance inequality was established using the inequalities of Fisher information. The established inequality was confirmed by numerical results which also satisfied the popular Cramer-Rao inequality. The theoretic impetuses for Fisher information, variance and Shannon entropy respectively, were calculated and their variation with some potentials were studied.

Keywords: Bound state; Wave equation; Eigensolutions; Fisher information; Shannon entropy.

Pac No: 03.65.Pm; 03.65.Ge; 03.65.Fd; 02.30.Gp.

* Corresponding author: oaclems14@physicist.net.

1. INTRODUCTION

In quantum mechanics, the only non-relativistic wave equation is the Schrödinger equation which has time-independent and time-dependent counterpart. In most cases, authors studied the time-independent counterpart of the Schrödinger equation with various potential models of interest in the space coordinate and obtained energy eigenvalue equation and the corresponding un-normalized radial wave functions. The time-like counterpart of the Schrödinger equation with time-dependent vector potential was derived by Horodecki from the relativistic Feinberg equation [1, 2]. This equation is called Feinberg-Horodecki equation though not adequately reported but known to be very useful in sciences. For instance, the time-like solution of the Feinberg-Horodecki equation with harmonic vector potential was used to test the relevance of the potential in physics, biology and medicine [3]. The Feinberg-Horodecki equations with different vector potentials have been used in the study of coherent states [4-7]. The notable equation was also used by Molski to interpret the formation of a specific growth pattern during the process of crystallization. It has also been shown that the space-like quantum system of the Feinberg-Horodecki equation, explain the mass in stable particle, the source of electric charge and the force between the electric charges [3, 8].

In recent time, few authors studied the quantized momentum as the solutions of the Feinberg-Horodecki equation for time-dependent vector potentials in one-dimensional system [9-11]. However, Eshghi et al. [10], studied Feinberg-Horodecki states of time-dependent mass distribution harmonic oscillator and obtained energy spectrum in one-dimensional case. The time-dependent Feinberg-Horodecki equation is given by

$$\left[-\frac{\hbar^2}{2\mu c^2}\frac{d^2}{dt^2}+V(t)-cP_n\right]R_n(t)=0, \tag{1}$$

where c the speed of light, t is the time point, $V(t)$ is the vector potential, μ is the reduced mass of particle and P_n is the quantized momentum. In the present study, we intend to determine the approximate solutions of the time-dependent one-dimensional Feinberg-Horodecki equation with a time-dependent harmonic vector potential. We also intend to calculate the impetuses of Fisher information and variance under Feinberg-Horodecki equation which has not been studied yet. The time-dependent harmonic vector potential is given by

$$V(t) = \frac{At^2}{2} \tag{2}$$

In the above potential, t is the time point, $A = m\omega^2$ and $\omega = 2\pi f$. The m is mass of the spring and f is the frequency of vibration. The harmonic potential describes the exact equation of motion and the approximate dynamics of the system. This paper is mainly segmented into two parts. The first part is the time-dependent solution of Feinberg-Horodecki equation. The second part is the calculation of the ratio of Fisher impetus to length, variance impetus to length and derivation of new variance inequalities.

2. Exact solutions of Feinberg-Horodecki Equation with Harmonic Vector Potential.

To obtain the quantized momentum of the system, we simply substitute equation (2) into equation (1) to have

$$-\frac{\hbar^2}{2mc^2}\frac{d^2R(t)}{dt^2} = \left[cP_n - \frac{At^2}{2} - \frac{\hbar^2}{2mc^2}\frac{\ell(\ell+1)}{t^2}\right]R(t), \tag{3}$$

where we have included $\frac{\ell(\ell+1)}{t^2}$ in equation (3) in order to determine the approximate solutions of Feinberg-Horodecki equation for any ℓ – state. In this paper, the authors want to use the methodology of parametric Nikiforov-Uvarov method to obtain the solutions of Eq. (3). Following the work of Tezcan and Sever [12], a standard form of second-order differential equation for parametric Nikiforov-Uvarov method is given as

$$\frac{d^2\psi(s)}{ds^2} + \frac{c_1 - c_2 s}{s(1-c_3 s)}\frac{d\psi(s)}{ds} + \frac{-\xi_0 s^2 + \xi_1 s - \xi_2}{s^2(1-c_3 s)^2}\psi(s) = 0. \tag{4}$$

With some mathematical manipulations and simplifications, Tezcan and Sever [12], came up with the condition for energy equation and its corresponding wave function as

$$c_2 n - (2n+1)c_5 + n(n-1)c_3 + c_7 + 2c_3 c_8 + (2n+1)\left(\sqrt{c_9} + c_3\sqrt{c_8}\right) + 2\sqrt{c_8 c_9} = 0, \tag{5}$$

$$\psi(s) = Ns^{c_{12}}(1-c_3 s)^{-c_{12}-\frac{c_{13}}{c_3}} P_n^{\left(c_{10}-1, \frac{c_{11}}{c_3}c_{10}-1\right)}(1-2c_3 s). \tag{6}$$

The parametric constants in Eq. (5) and Eq. (6) are deduce as follows

$$\left.\begin{aligned} &c_4=\frac{1-c_1}{2}, c_5=\frac{c_2-2c_3}{2}, c_6=c_5^2+\xi_1, c_7=2c_4c_5-\xi_2, c_8=c_4^2+\xi_3, \\ &c_9=c_3\left(c_7+c_3c_8\right)+c_6, c_{10}=c_1+2c_4+2\sqrt{c_8}, c_{11}=c_2-2c_5+2\left(\sqrt{c_9}+c_3\sqrt{c_8}\right), \\ &c_{12}=c_4+\sqrt{c_8}, c_{13}=c_5-\left(\sqrt{c_9}+c_3\sqrt{c_8}\right) \end{aligned}\right\}. \quad (7)$$

Substituting Eq. (2) into Eq. (3) and define a simple variable of the form $t=\sqrt{y}$, a parametric form of a one-dimensional Schrödinger equation is obtained in the form

$$\frac{d^2R_{n,\ell}(y)}{dy^2}+\frac{1}{2y}\frac{dR_{n,\ell}(y)}{dy}+\frac{-\frac{\mu c^2A}{4\hbar^2}y^2+\frac{\mu c^3P_n}{2\hbar^2}y-\frac{\ell(\ell+1)}{4}}{y^2}R_{n,\ell}(y)=0. \quad (8)$$

Comparing Eq. (8) with Eq. (4), the parametric constants in Eq. (7) are deduced as follows

$$\left.\begin{aligned} &c_1=\frac{1}{2}, c_2=c_3=0, c_4=\frac{1}{4}, c_5=0, c_6=\frac{\mu c^2A}{4\hbar^2}, c_7=-\frac{\mu c^3P_n}{2\hbar^2}, c_8=\frac{1}{16}+\frac{\ell(\ell+1)}{4}, \\ &c_9=\frac{\mu c^2A}{4\hbar^2}, c_{10}=\frac{3+2\ell}{2}, c_{11}=2\sqrt{\frac{\mu c^2A}{4\hbar^2}}, c_{12}=\frac{1+\ell}{2}, c_{13}=-\sqrt{\frac{\mu c^2A}{4\hbar^2}}. \end{aligned}\right\} \quad (9)$$

Substituting c_1 to c_9 into Eq. (5) and c_{10} to c_{13} into Eq. (6), we have the energy equation and the radial wave functions respectively for one dimensional Schrödinger equation as

$$P_{n,\ell}=\frac{2f}{\mu c^2}\sqrt{\mu m}\left(2n+\frac{3}{2}+\ell\right), \quad (10)$$

$$R_{n,\ell}(y)=Ny^{\frac{1+\ell}{2}}e^{-y\sqrt{\frac{\mu c^2A}{4\hbar^2}}}L_n^{\frac{1+2\ell}{2}}\left(y\sqrt{\frac{\mu c^2A}{\hbar^2}}\right). \quad (11)$$

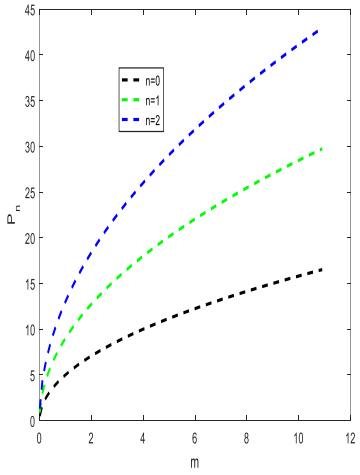

Figure 1: Quantized momentum against the mass of the spring at the ground state and the first two excited states.

3. INFORMATION-THEORETIC IMPETUSES AND LENGTHS

In this section, we obtain information-theoretic impetuses and length for Fisher information and Variance. To calculate these, we first calculate some expectation values, Fisher information and variance both for time point and momentum space. To calculate the expectation values using Hellmann-Faynman Theory (HFT) [13-19], when a Hamiltonian H for a given quantum system is a function of some parameters v, the quantized momentum $P_{n,\ell}(v)$ and eigenfunctions $R_{n,\ell}(v)$ of H are given by

$$\frac{\partial P_{n,\ell}(v)}{\partial v} = \left\langle R_{n,\ell}(v) \right| \frac{\partial H(v)}{\partial v} \left| R_{n,\ell}(v) \right\rangle, \tag{12}$$

with the effective Hamiltonian as

$$H = -\frac{\hbar^2}{2\mu}\frac{d^2}{dt^2} + \frac{\hbar^2}{2\mu}\frac{\ell(\ell+1)}{t^2} - 2m\pi^2 f^2 t^2. \tag{13}$$

Setting $v = m$ and $v = \mu$, we have the expectation values of t^2 and p^2 as

$$\left\langle t^2 \right\rangle_{n,\ell} = \frac{\hbar\mu\left(2n + \frac{3}{2} + \ell\right)}{2\pi f c^2 \sqrt{\mu m}}. \tag{14}$$

$$\left\langle p^2 \right\rangle_{n,\ell} = \frac{\hbar\pi\left(2n + \frac{3}{2} + \ell\right) mf}{\mu c^2 \sqrt{\mu m}}. \tag{15}$$

(i): Fisher Information.

Following the works of Dehesa et al., Romera et al., and Onate et al. [20-22] respectively, the time and momentum Fisher information are given as

$$I(\rho) = 4\left\langle p^2 \right\rangle_{n,\ell}, \tag{16}$$

$$I(\gamma) = 4\left\langle t^2 \right\rangle_{n,\ell}, \tag{17}$$

Using Eq. (14) and Eq. (15), the Fisher information in Eq. (16) and Eq. (17) respectively become

$$I(\rho) = \frac{2\hbar\pi\left(4n + 3 + 2\ell\right) mf}{\mu c^2 \sqrt{\mu m}}, \tag{18}$$

$$I(\gamma)=\frac{\hbar\left(4n+3+2\ell\right)}{\pi fc^2\sqrt{\mu m}}. \tag{19}$$

Having obtained the Fisher information for both time and momentum, we can now calculate the ratio of Fisher impetus to length. The ratio of Fisher impetus to length is defined as [23]

$$F_{I(\rho,\gamma)}=\frac{F_I}{F_L}=\sqrt{\frac{I(\rho)}{I(\gamma)}}=\sqrt{\frac{4\left\langle p^2\right\rangle}{4\left\langle r^2\right\rangle}}\,. \tag{20}$$

Substituting Eq. (18) and Eq. (19) into Eq. (20), we deduce the ratio of Fisher impetus as follows:

$$F_{I(\rho,\gamma)}=f\pi\sqrt{\frac{2m}{\mu}}. \tag{21}$$

(ii): Variance.

Following the paper of Dehesa et al. [24], time variance under information theoretic measure is given by

$$V(\rho)=\frac{1}{4}I(\gamma), \tag{22}$$

while that of the momentum space is given by

$$V(\gamma)=\frac{1}{4}I(\rho). \tag{23}$$

Substituting Eq. (14) and Eq. (15) respectively into Eq. (22) and Eq. (23), we have time variance and momentum variance respectively as

$$V(\rho)=\frac{\hbar\left(2n+\frac{3}{2}+\ell\right)}{2\pi fc^2\sqrt{\mu m}}., \tag{24}$$

$$V(\gamma)=\frac{\hbar\pi\left(2n+\frac{3}{2}+\ell\right)mf}{\mu c^2\sqrt{\mu m}}. \tag{25}$$

The ratio of Variance impetus to length is defined as

$$V_{I(\rho,\gamma)}=\sqrt{\frac{V(\rho)}{V(\gamma)}}\,. \tag{26}$$

Substituting Eq. (24) and Eq. (25) into Eq. (26), we have

$$V_{I(\rho,\gamma)} = \frac{1}{\pi f}\sqrt{\frac{\mu}{2m}}. \tag{27}$$

(iii) Shannon Entropy.

Shannon entropy for position space and momentum space respectively are given as

$$S(\rho) = -\int \rho(r) log\, \rho(r) dr, \tag{28}$$

$$S(\gamma) = -\int \gamma(p) log \gamma(p) dp, \tag{29}$$

where $\rho(r)$ and $\gamma(p)$ corresponds to the wave function $R(r)$ and $R(p)$ respectively for position space and momentum space. According to Dehesa et al. [25], the Shannon entropies of the harmonic oscillator for one dimension at the ground state are given as

$$S(\rho) = \frac{1}{2}\left(1 + log\pi - log(2\pi mf)\right), \tag{30}$$

$$S(t) = \frac{1}{2}\left(1 + log\pi + log(2\pi mf)\right). \tag{31}$$

At the first excited state, these authors gave these entropies as

$$S(\rho) = C + 2log2 - \frac{1}{2}\left(log(2\pi mf) + 1 + log\frac{4}{\pi}\right), \tag{32}$$

$$S(t) = C + 2log2 + \frac{1}{2}\left(log(2\pi mf) - 1 - log\frac{4}{\pi}\right), \tag{33}$$

where C is the Euler's constant with numerical value as 0.5772156649.

The ratio of Variance impetus to length is defined as

$$S_{I(t,\rho)} = e^{\sqrt[3]{S(t)-S(\rho)}}. \tag{34}$$

Substituting Eq. (32) and Eq. (33) into Eq. (34), we have

$$S_{I(t,\rho)} = exp\left(\sqrt[3]{log(2\pi mf)}\right). \tag{35}$$

(iv) Uncertainty Relations

Here, we want to introduce an uncertainty relations/inequalities for variance. The relations/inequalities here will be established base on the Cramer-Rao inequalities for the Fisher information. It is shown from Cramer-Rao inequalities that

$$\left.\begin{aligned} I(\rho) &\geq \frac{9}{\langle t^2 \rangle} \\ I(\gamma) &\geq \frac{9}{\langle p^2 \rangle} \end{aligned}\right\}. \tag{36}$$

Manipulating Eq. (16) and Eq. (17) and relate it to Eq. (36), we can write

$$\langle p^2 \rangle \langle r^2 \rangle \geq \frac{81}{16} \frac{\langle p^2 \rangle \langle r^2 \rangle}{\left(\langle p^2 \rangle \langle r^2 \rangle \right)^2}. \tag{37}$$

Using Eq. (22) and Eq. (23) in Eq. (37), we have

$$V(\rho)V(\gamma) \geq \frac{9}{4}. \tag{38}$$

Eq. (38) gives a boundary condition that the product of variance cannot go beyond 9/4. Manipulating Eq. (38) further, we have another relation of the form

$$16V(\rho)V(\gamma) \geq 36. \tag{39}$$

Eq. (39) shows that the product of variance and sixteen can never go beyond 36. The variance uncertainty inequality of Eq. (39) when transform to the popular Fisher information inequality, is equivalent to Eq. (29) of Ref [24] written as

$$I(\rho)I(\gamma) \geq 36 \tag{40}$$

The accuracy of Eq. (38) and Eq. (40) will numerically be verified.

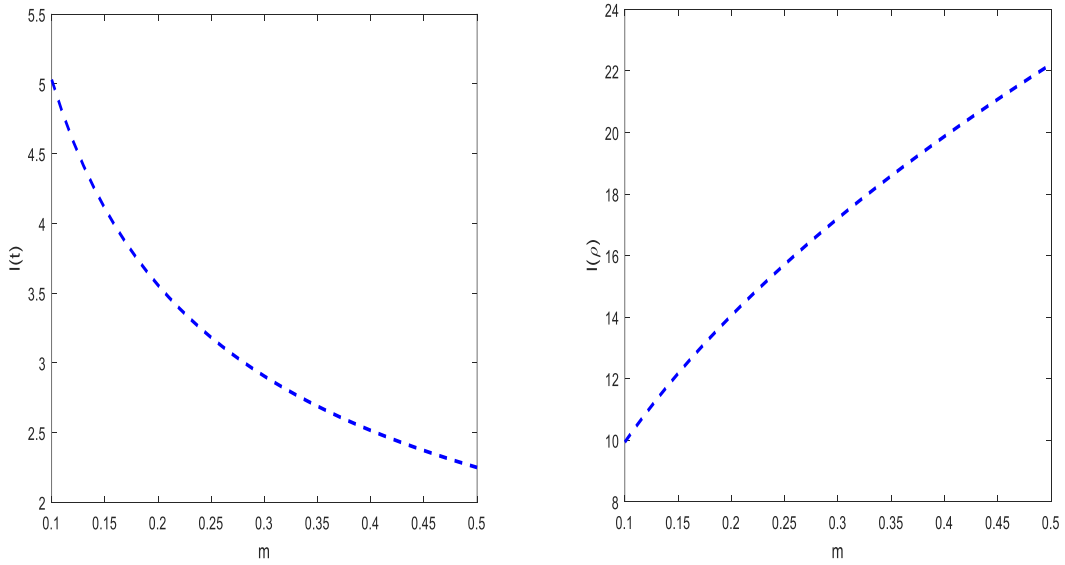

Figure 2: The variation of time Fisher information $I(\gamma)$ and momentum Fisher information $I(\rho)$ respectively against mass m of the spring.

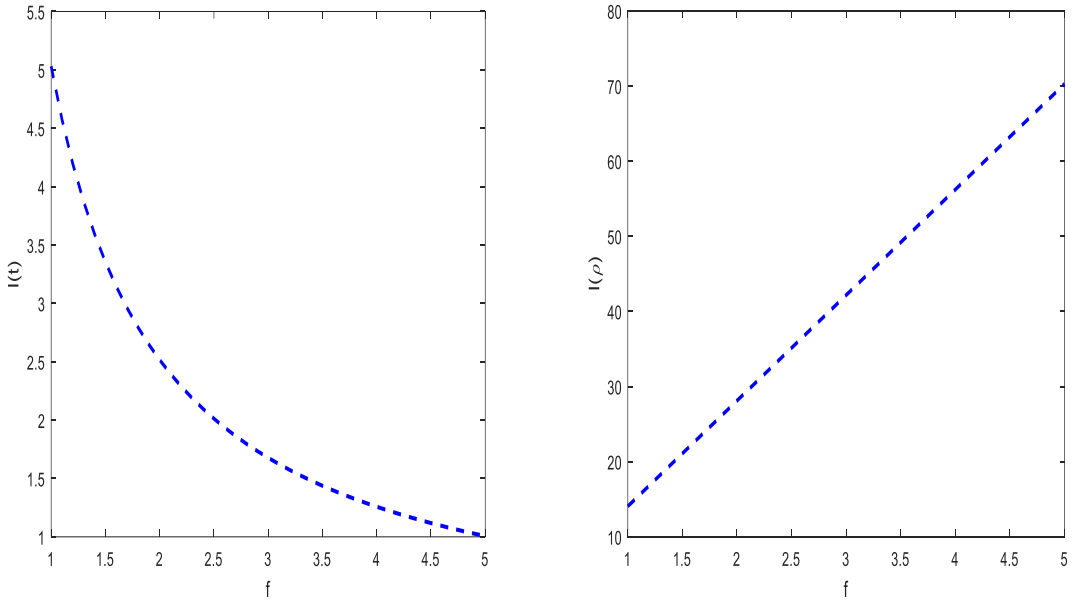

Figure 3: Time Fisher information $I(t)$ and momentum Fisher information $I(\rho)$ against frequency f .

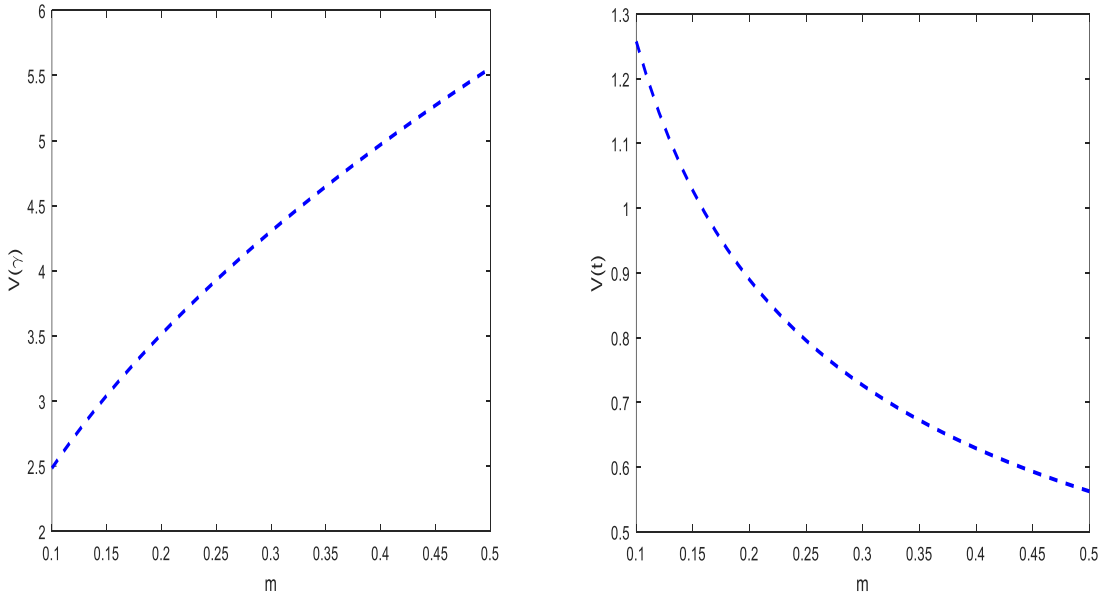

Figure 4: Variation of the momentum Variance $V(\gamma)$ and the time variance $V(t)$ against the mass m of a spring.

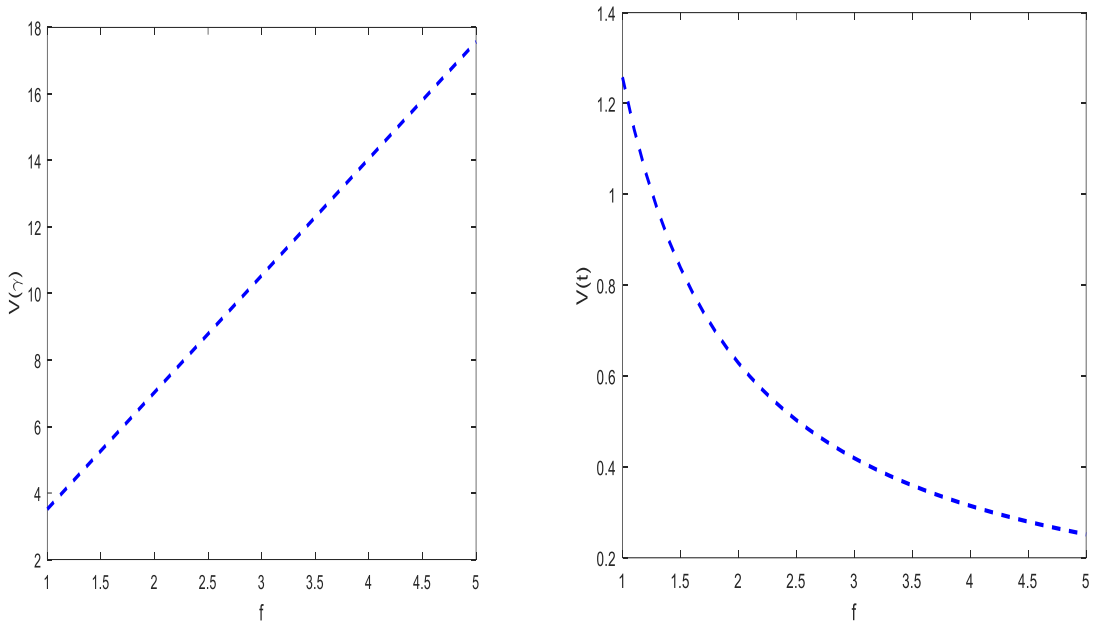

Figure 5: Variation of momentum variance and time variance respectively against frequency.

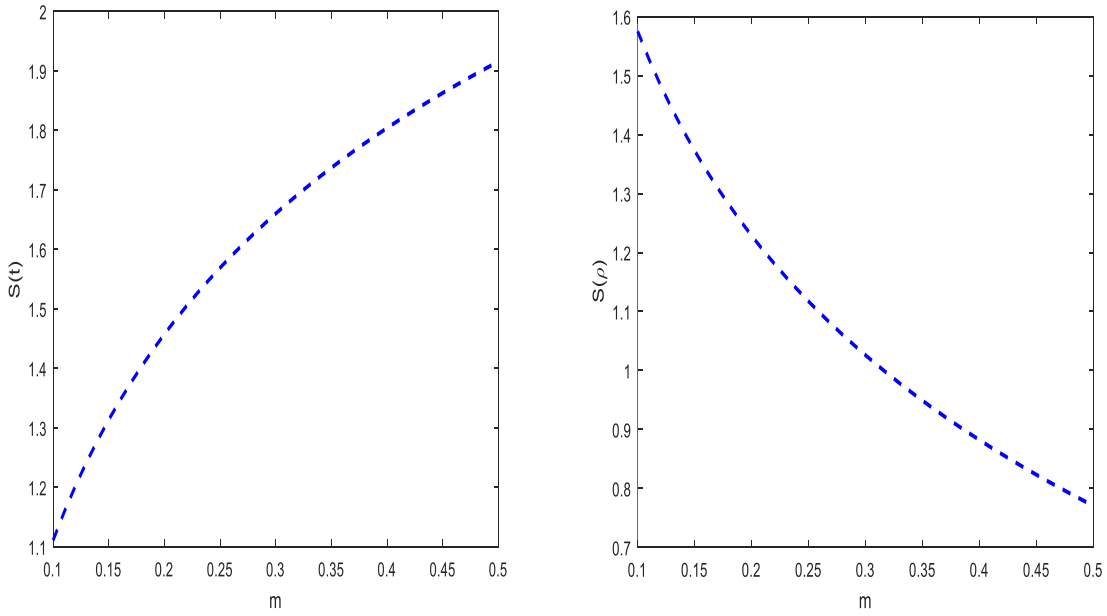

Figure 6: The variation of time Shannon entropy $S(t)$ and momentum Shannon entropy $S(\rho)$ respectively against mass m of the spring.

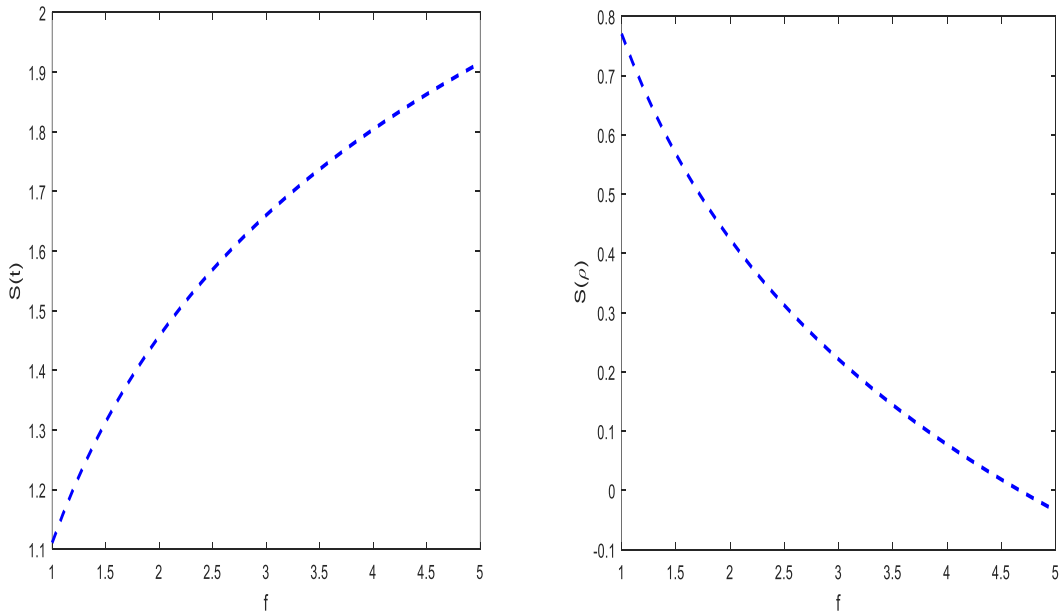

Figure 7: Time Shannon entropy $S(t)$ and momentum Shannon entropy $S(\rho)$ against frequency f .

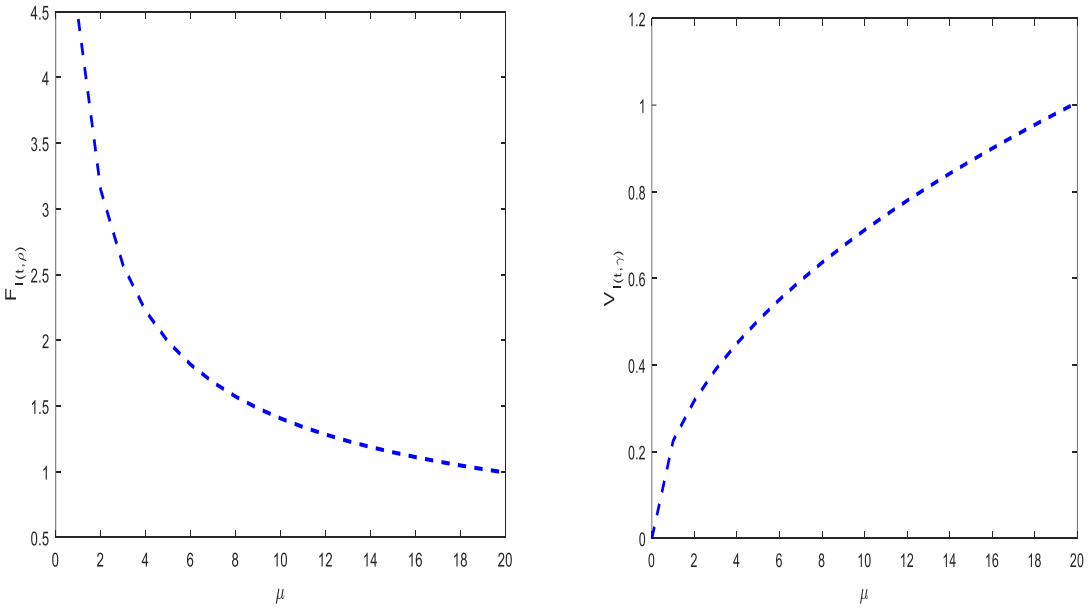

Figure 8: The variation of the ratio of Fisher impetuses $F_{I(t,\rho)}$ and Variance impetuses $V_{V(t,\gamma)}$ respectively against the reduced mass μ

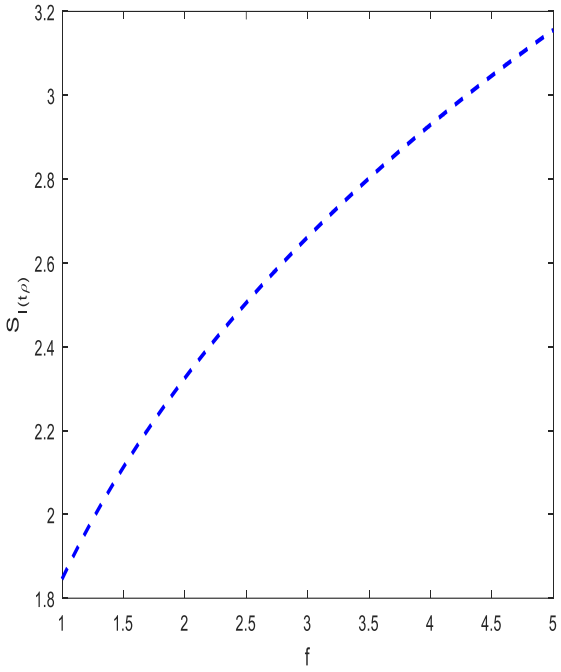

Figure 9: The variation of the ratio of Shannon impetuses $S_{I(t,\rho)}$ against the frequency f.

Table 1: Numerical values for Fisher and Variance inequalities.

m	$\langle t^2 \rangle$	$\langle p^2 \rangle$	$\langle t^2 \rangle \langle p^2 \rangle$	$16\langle t^2 \rangle \langle p^2 \rangle$	$81/\langle t^2 \rangle \langle p^2 \rangle$
1	0.397727273	7.857142857	3.125000002	50.00000000	25.91999998
2	0.281235652	11.11167799	3.125000004	50.00000032	25.91999998
3	0.229627948	13.60897063	3.125000000	50.00000006	25.92000000
4	0.198863636	15.71428571	3.124999993	49.99999989	25.92000006
5	0.177869044	17.56910554	3.125000006	50.00000000	25.91999995
6	0.162371479	19.24599084	3.124999998	49.99999997	25.92000002

Table 2: Numerical results of Shannon entropy for BBM inequality.

m	$S(\rho)$	$S(\gamma)$	$S(\rho)+S(\gamma)$
1	0.423789255	2.2620687400	2.685857995
2	0.077215665	2.6086423303	2.685857995
3	-0.125516889	2.8113748844	2.685857995
4	-0.269357925	2.9552159206	2.685857995
5	-0.380929701	3.0667876963	2.685857995
6	-0.472090479	3.1579484747	2.685857995

4. **DISCUSSION**

In Figure 1, the effect of the mass of the spring on the quantized momentum for three different quantum states was shown. An increase in the mass of the spring brings an increase in the quantized momentum. The quantized momentum at different states diverges as the mass increases. The variation of time Fisher information $I(t)$ and momentum Fisher information $I(\rho)$ respectively against mass (m) of the spring were shown in Figure 2. The time Fisher information goes down monotonically as the mass of the spring increases. The momentum Fisher information rises significantly as the mass of the spring increases. This physically means that a more concentration of the electron density in the time Fisher information correspond to a less concentration of electron density in the Fisher information for momentum space and vice visa. Figure 3 showed time Fisher information $I(t)$ and momentum Fisher information $I(\rho)$ against frequency f . As the frequency increases, the time Fisher information decreases monotonically while the momentum Fisher information increases linearly. This simply means that the momentum Fisher information has smaller uncertainty, hence a few time will be spent to predict the accuracy of localizing the position of a particle in a system. On the other hand, the time Fisher information has more uncertainty and as such more time will be spent to predict the localization of a particle in a system. The variation of the momentum Variance $V(\gamma)$ and the time variance $V(t)$ against the mass m of a spring were shown in Figure 4. When the mass increases gradually, the momentum variance also increases almost linearly while the time variance decreases monotonically. This simply indicates that a diffused density distribution in the time configuration, associated with a localized density distribution in the momentum counterpart. However, the minimum variance in each case is seen to be bounded above negative. Figure 5 presented the variation of momentum variance and time variance respectively against frequency. As the frequency increases from one (1), there is an inverse relationship between the momentum variance and the time variance. Thus, a strongly localized distribution in the time density corresponds to a widely delocalized density in the momentum configuration and vice visa. Figure 6 showed the variation of time Shannon entropy and momentum Shannon entropy against the mass of the spring. An increase in the time Shannon entropy corresponds to a decrease in the momentum Shannon entropy as the

mass of the spring increases. At the 0.1 to 0.5 values of the mass of the spring, the Shannon entropy for both cases are bounded above negative.

The variation of the time Shannon entropy and momentum Shannon entropy respectively against the frequency were presented in Figure 7. A strongly localized distribution in the time density corresponds to a widely delocalized density in the momentum configuration and vice visa as the frequency of vibration rises gradually. In the momentum Shannon entropy, an entropy squeezing was noticed. The squeezing effect becomes more as the frequency increases. Figure 8 are plots for the ratio of Fisher impetuses $F_{I(\gamma,\rho)}$ and Variance impetuses $V_{V(\gamma,\rho)}$ respectively against the reduced mass m. An increase in the reduced mass results to an increase in the variance impetuses but a decrease in the Fisher impetuses. The ratio of Shannon impetuses is shown in Figure 9. As the frequency of vibration increases gradually, the ratio of Shannon impetuses rises. Table 1 presents numerical values for the expectation values and their products. The excess of this Table is to verify the accuracy of the relations (inequalities) given in Eq. (38) and Eq. (40). From the Table, the minimum value of the product of the variance is 3.124999998. This value is seen to be greater than 9/4 (2.25). Thus, Eq. (38) is justified. Similarly, the minimum value of the product of sixteen and the product of the expectation values is 49.99999997. This value is also seen to be greater than 36. This also confirmed the correctness of Eq. (39). In Table 2, the numerical values for Shannon entropy was presented using Eq. (32) and Eq. (33) respectively. The main aim of Table 2 is to verify the accuracy of Bialynick-Birula, Mycielski (BBM) inequality; $S(t)+S(\rho)\geq 1+log\pi$. This inequality is the major check of the accuracy for the computation of Shannon entropy. It simply means that the sum of the time Shannon entropy and momentum Shannon entropy can never go beyond sum of one and the log of π. From the table the sum of the entropies remain constant (2.685857995) for all values of the frequency. This value is greater than that $1+log\pi$ (1.497149872). Thus, the accuracy of the Shannon entropies were verified in Table 2.

5. CONCLUSION

A one-dimensional time dependent Feinberg-Horodecki equation for the time-dependent harmonic vector potential was calculated using parametric Nikiforov-Uvarov method. The behaviour of Fisher information under the Feinberg-Horodecki equation is similar to that in the energy eigenvalues for one dimensional systems. It is deduced that the impetuses of the Fisher information and that of the variance are inversely related. However, the variation of

the impetuses of variance and that of the Shannon entropy are similar. The numerical values for the sum of Shannon entropy for all values of the frequency remains constant as the results confirmed BBM inequality.

Declarations
Funding: N/A
Conflict of interest/Competing interest: N/A
Availability of data and material: N/A
Code availability: N/A
Authors' contributions:
C.A. Onate; Formulate the work, solved the calculations
D.T. Bankole; Wrote the introduction
A.S. Olayinka; Discussed the results
O.E. Odeyemi; Makes all the plots and wrote the conclusion.

REFERENCES

[1] Horodecki R (1988). Extended wave description of a massive spin-0 particle. Nuovo Cim. B 102, 27-32.

[2] Feinberg G (1976). Possibility of Faster-Than-Light Particles. Phys. Rev. 159, 1089-1105.

[3] Molski M (2006). Space-like coherent states of time-dependent Morse oscillator. Eur. Phys. J. D 40, 411-416.

[4] Levine RD (1985). Dynamical symmetries**.** J. Phys. Chem. 89, 2122-2129.

[5] Benedict MG, Molnar B (1999). Algebraic construction of the coherent states of the Morse potential based on supersymmetric quantum mechanics. Phys. Rev. A 60, 1737-1743.

[6] Neioto M, Simmons LM (1979). Coherent states for general potentials. I. Formalism. Phys. Rev. D 20, 1321-1331.

[7] Fukui T, Aizawa A (1999). Shape-invariant potentials and an associated coherent state. Phys. Rev. A 180, 308-313.

[8] Hamzavi M, Ikhdair SM, Amirfakhrian M (2013). Exact solutions of Feinberg-Horodecki equation for time-dependent Deng-Fan molecular potential. J. Theor. Phys. 7, 40.

[9] Arda A, Sever R (2017). Feinberg-Horodecki equation with Pôschl-Teller potential: Space-like coherent states. arXiv:1704.02976v2 [quant-ph] 2017.

[10] Eshghi M, Sever R, Ikhdair SM (2016). Feinberg-Horodecki states of a time-dependent mass distribution harmonic oscillator. Eur. Phys. J. Plus 131**,** 223.

[11] Ojonubah JO, Onate CA (2016). Exact solution of the Feinberg-Horodecki equation for time-dependent Tietz-Wei diatomic molecular potential. Afr. Rev. Phys. 10, 453-456 (2016).

[12] C. Tezcan, R. Sever, A General Approach for the Exact Solution of the Schrödinger equation, Int. J. Theor. Phys. 48 337-350 (2009).
[13] G. Hellmann. Einfuhrung in die Quantenchemie (Denticke, Vienna, 1937)

[14] R.P. Feynman, Forces in Molecules. Phys. Rev. 56, 340 (1939).

[15] Oyewumi JK (2005). Analytical solutions of the Kratzer-Fues potential in an arbitrary number of dimensions. Found. Phys. Lett. 18, 75-84.

[16] Onate CA (2013). Relativistic and non-relativistic solutions of the inversely quadratic Yukawa potential. Afr. Rev. Phys. 8, 325-329.

[17] Popov D (2001). Barut-Girardello coherent states of the pseudoharmonic oscillator. J. Phys. A: Math. Gen. 34, 5283.

[18] Hassanabadi H, Yazarloo BH, LU LL (2012). Approximate Analytical Solutions to the Generalized Pöschl—Teller Potential in *D* Dimensions. Chin. Phys. Lett. 29, 020303.

[19] Oyewumi KJ, Sen KD (2012). Exact solutions of the Schrödinger equation for the pseudoharmonic potential: an application to some diatomic molecules. J. Math. Chem. 50, 1039-1059.

[20] Dehesa JS, Gonzalez-Ferez R, Sanchez-Moreno P (2007). The Fisher-information-based uncertainty relation, Cramer–Rao inequality and kinetic energy for the *D*-dimensional central problem. J. Phys. A: Math. Theor. 40 1845.

[21] Romera E, Sanchez-Moreno P, Dehesa JS (2005). The Fisher information of single-particle systems with a central potential. Chem. Phys. Lett. 414, 468472.
[22] Onate CA, Onyeaju MC, Ikot NA, Ebomwonyi O, Idiodi JOA (2019). Fisher information and uncertainty relations for potential family. Int. J. Quant. Chem. 119, e25991.

[23] Yahya WA, Oyewumi KJ, Sen KD (2015). Position and momentum information-theoretic measures of the pseudoharmonic potential Int. J. Quant. Chem. 115, 1543-1552.

[24] Dehesa JS, Martinez-Finkelshtein A, Sorokin VN (2006). Information theoretic measures Morse and Pöschl-Teller potentials. Molecular Phys. 104, 613-622.

[25] Dehesa JS, Assche WV, Yáñez RJ (1997). Information entropy of classica orthogonal polynomials and their application to the harmonic oscillator and Coulomb potentials. Meth. Appl. Analysis 4, 91-110.